Electronic Supplementary Information

Activating surface and bulk of hematite photoanodes to boost solar water splitting

Hemin Zhang,[a] Jong Hyun Park,[b] Woo Jin Byun,[a] Myoung Hoon Song,[b] Jae Sung Lee[a,*]

[a]School of Energy and Chemical Engineering, Ulsan National Institute of Science and Technology (UNIST), 50 UNIST-gil, Ulsan 44919 (Republic of Korea)

[b]Perovtronics Research Center, Ulsan National Institute of Science and Technology (UNIST), 50 UNIST-gil, Ulsan, 44919 Republic of Korea.

Corresponding Author

*E-mail (Jae Sung Lee): jlee1234@unist.ac.kr

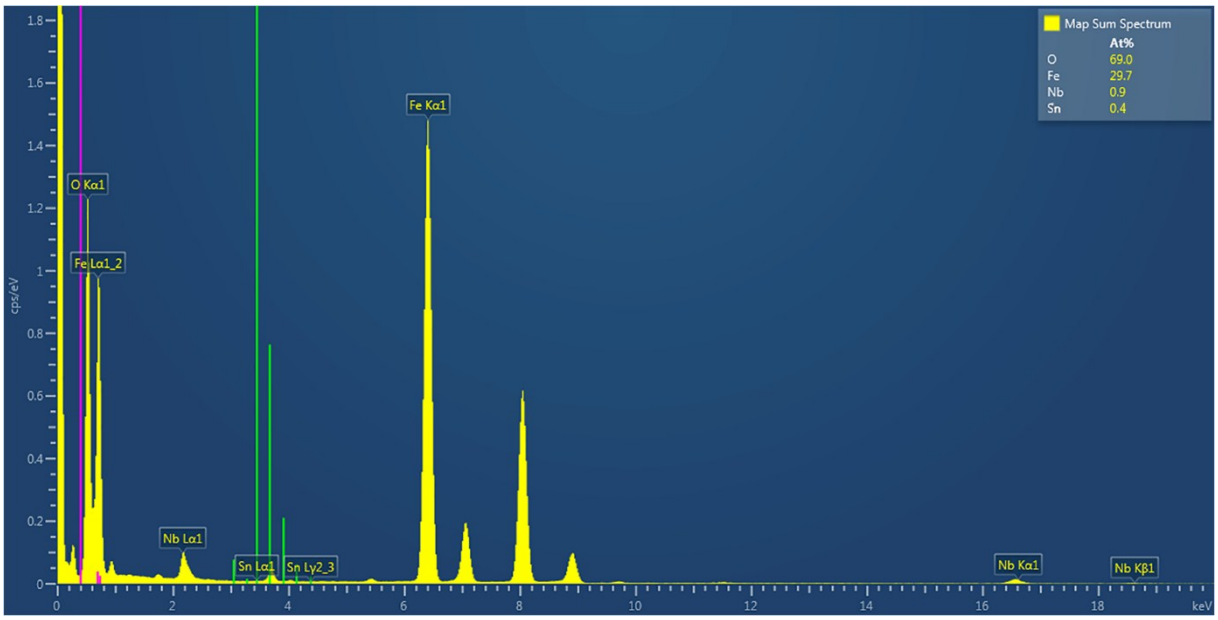

Fig. S1 EDX spectrum of hematite nanorods with dual dopants of Nb and Sn.

a 20181205-1@720/725/730/735-ES@Quant@. All Data Report 12/5/2018, 3:23:14 PM

Fe 238.204 Calibration (mg/kg) **12/5/2018, 10:47:23 AM** **Correlation Coefficient: 0.999998**

Label	Flags	Int. (c/s)	Std Conc.	Calc Conc.	Error	%Error
Blank		4.63	0.000	0.000	-	-
Standard 1		25505	1.00	1.02	0.018	1.8
Standard 2		125131	5.00	4.99	-0.006	-0.1
Standard 3		250596	10.0	10.0	0.001	0.0

Curve Type: Linear Equation: y = 25055.9 x + 4.6

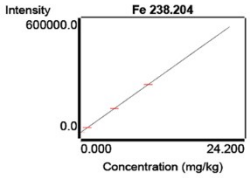

#1 (Samp) **12/5/2018, 10:34:13 AM** **Tube 24**

Weight: 0.0002 **Volume: 50** **Dilution: 1**

Label	Sol'n Conc.	Units	SD	%RSD	Int. (c/s)	Calc Conc.	DF
Fe 238.204	1.91	mg/kg	0.039	2.0	47832	477210 mg/kg	1.00

b 20181205-2@720/725/730/735-ES@Quant@. All Data Report 12/5/2018, 3:22:45 PM

Nb 309.417 Calibration (mg/kg) **12/5/2018, 11:33:37 AM** **Correlation Coefficient: 0.999993**

Label	Flags	Int. (c/s)	Std Conc.	Calc Conc.	Error	%Error
Blank		13.9	0.000	0.000	-	-
Standard 1		6577	1.00	0.979	-0.021	-2.1
Standard 2		33348	5.00	4.97	-0.028	-0.6
Standard 3		67157	10.0	10.0	0.016	0.2

Curve Type: Linear Equation: y = 6703.6 x + 13.9

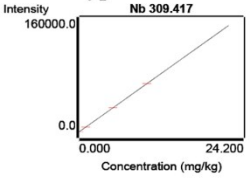

#1 (Samp) **12/5/2018, 11:39:03 AM** **Tube 11**

Weight: 0.0002 **Volume: 50** **Dilution: 1**

Label	Sol'n Conc.	Units	SD	%RSD	Int. (c/s)	Calc Conc.	DF
Nb 309.417	0.128	mg/kg	0.003	2.2	869	26218 mg/kg	1.00

Fig. S2 The concentration of Nb is 5.5 wt% by ICP-OES, which is consistent with the result of TEM-EDX (0.9 at%~5.2 wt%).

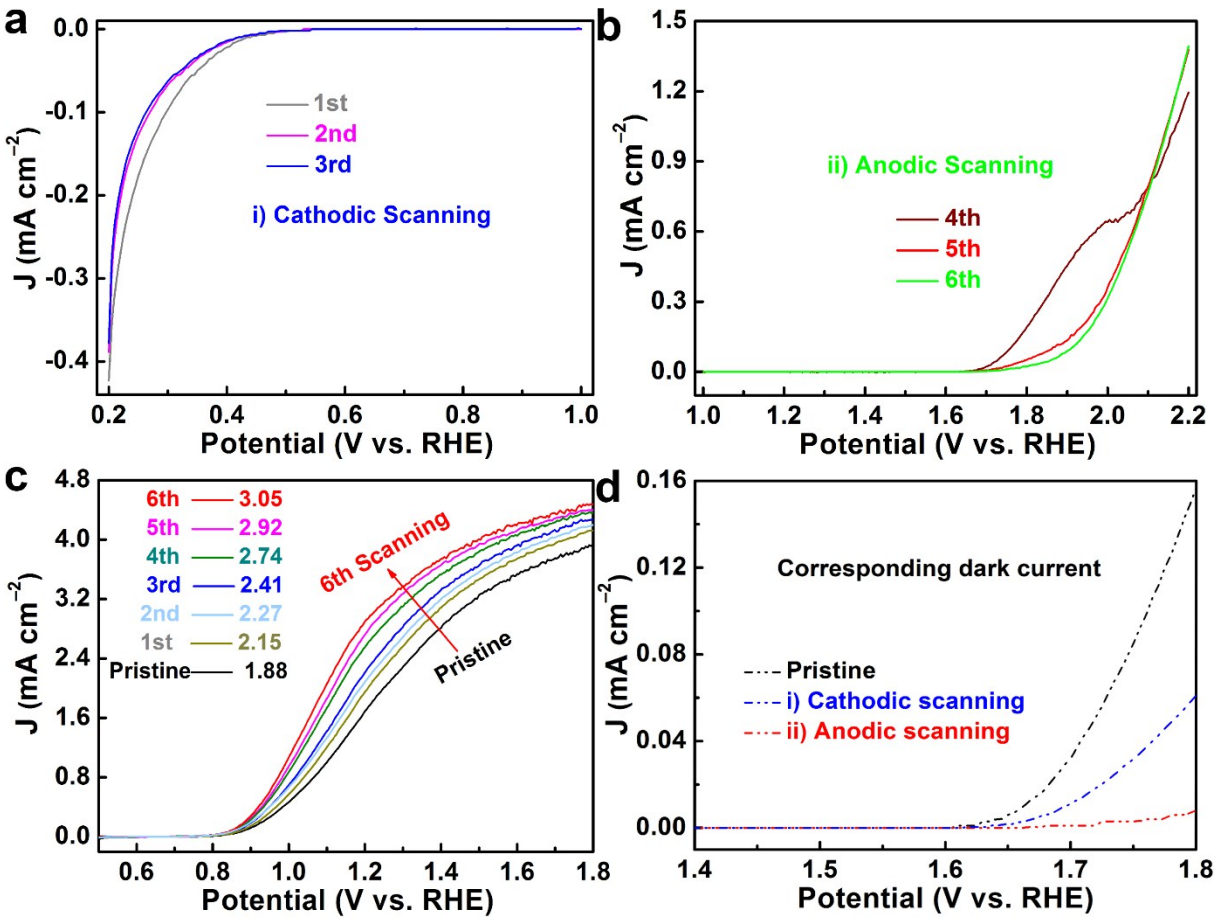

Fig. S3 Electrochemical activation process: a thrice cathodic scanning (a) and a following thrice anodic scanning (b). The corresponding *J–V* curves (c) and dark current density (d). The trend of activating treatment is that both first reduction (1st anodic scanning) and oxidation (4th cathodic scanning) scannings are much effective to improve photocurrent relative to the following scannings. This is reasonable because the first anodic/cathodic scanning in a certain (optimum) potential range will induce almost all the reactions that easily occurr, and the following 2nd and 3rd ones will realize a little more difficult reactions. More scannings in a certain (optimum) potential range cannot improve the photocurrent further. During the process of cathodic and anodic scanning, the dark currents of the water reduction and oxidation reactions are suppressed, indicating that some active sites on the surface of hematite photoanode were removed. On this basis, we rule out the enhancement of photocurrent densities of the activated films being a result of a higher concentration of active sites. Notably, there is an obvious shoulder between the first anodic scanning (the 4th scanning) and the second anodic scanning (the 5th scanning), which suggests that some oxidation occurred in the photoelectrode after cathodic reduction.

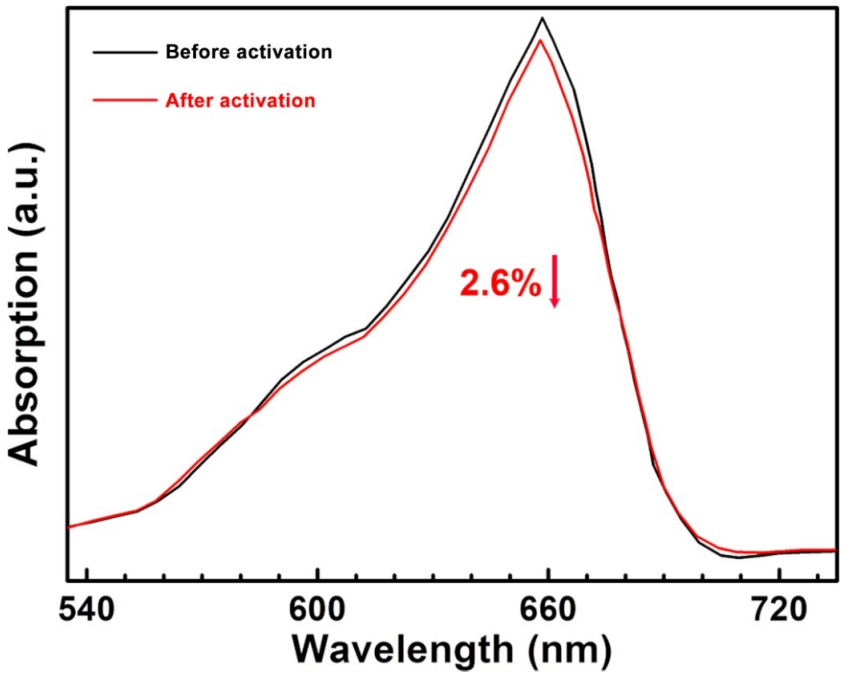

Fig. S4 Absorption spectra from the desorbed methylene blue dye molecules using geometric area of hematite nanorod films (1 cm^2) before and after activation treatment. The samples with and without activation were immersed into 0.1 mM L^{-1} methylene blue aqueous solution for 24 h. Subsequently, the samples were dipped into deionized water for 2 min, then taken out and dried by nitrogen. Each sample was immersed into the same volume of acetonitrile for 20 min to make desorption of methylene blue molecules. The characteristic absorbance peak at ~655 nm is a good indicator of the amount of desorbed molecules, which indirectly confirms the surface area of hematite nanorods.[1]

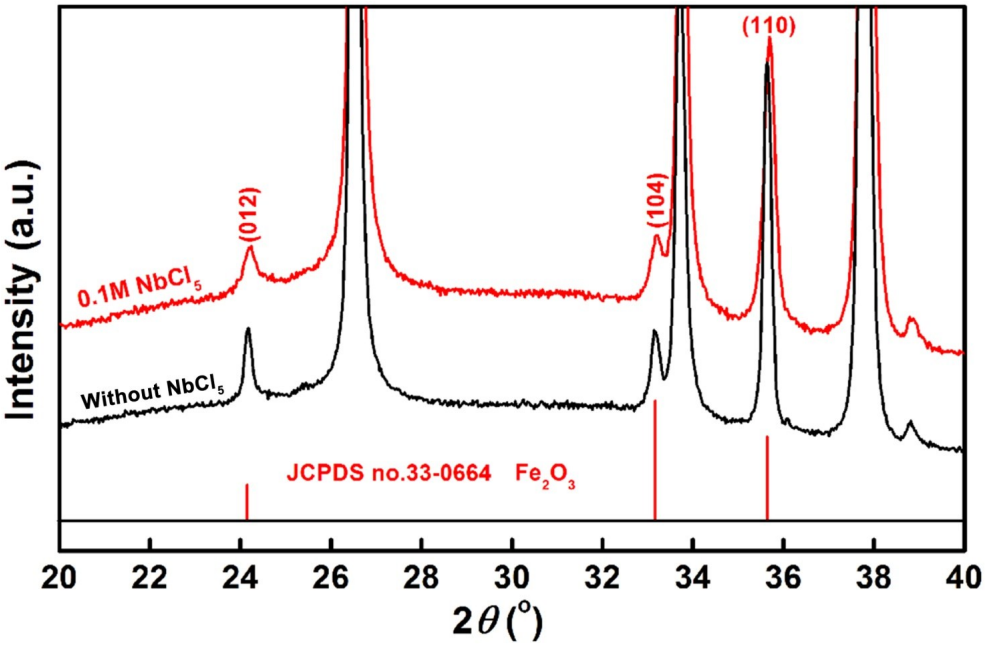

Fig. S5 XRD spectra with and without 0.1 M $NbCl_5$, finally forming Nb, Sn co-doped and Sn doped hematite nanorods, respectively.

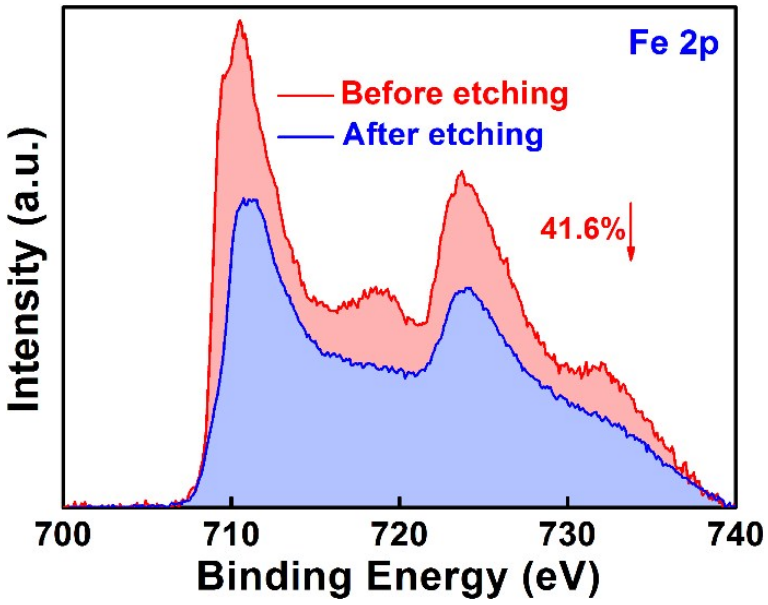

Fig. S6 Calculation of the increased intensity by integration of peak areas.

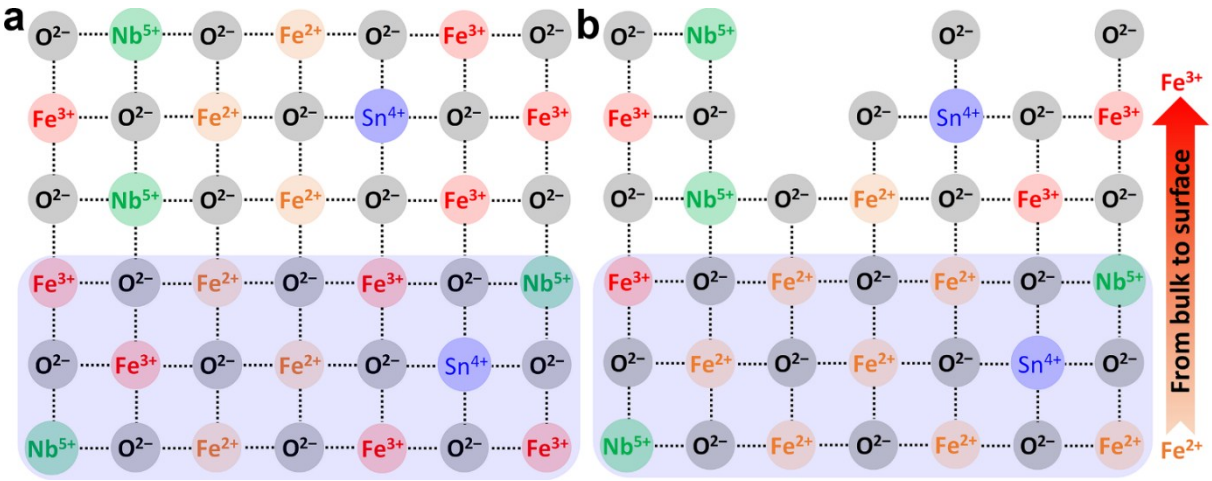

Fig. S7 Schematic illustration for surface and bulk of elemental variation before (a) and after (b) the electrochemical activation treatment.

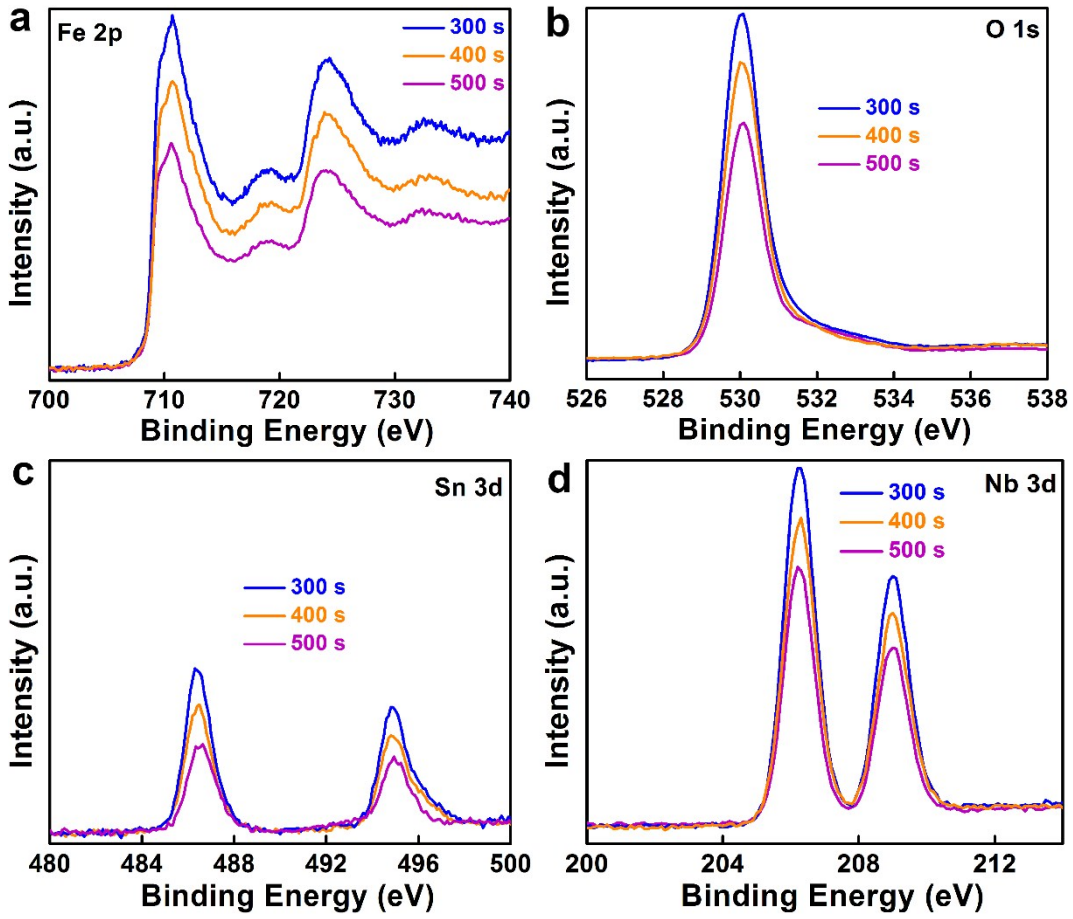

Fig. S8 The prolonged depth profiling for the pristine sample.

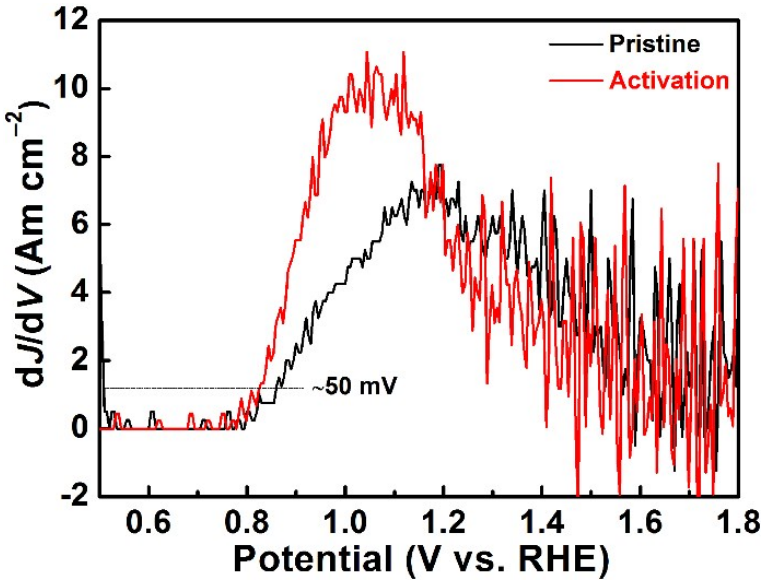

Fig. S9 Onset potential estimated by plotting the first order derivative of the photocurrent density against the voltage.

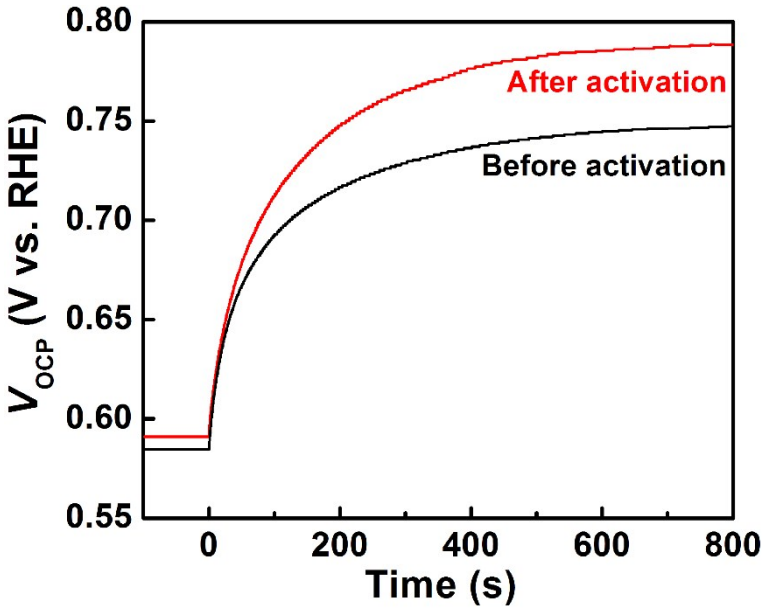

Fig. S10 photovoltage before and after activation.

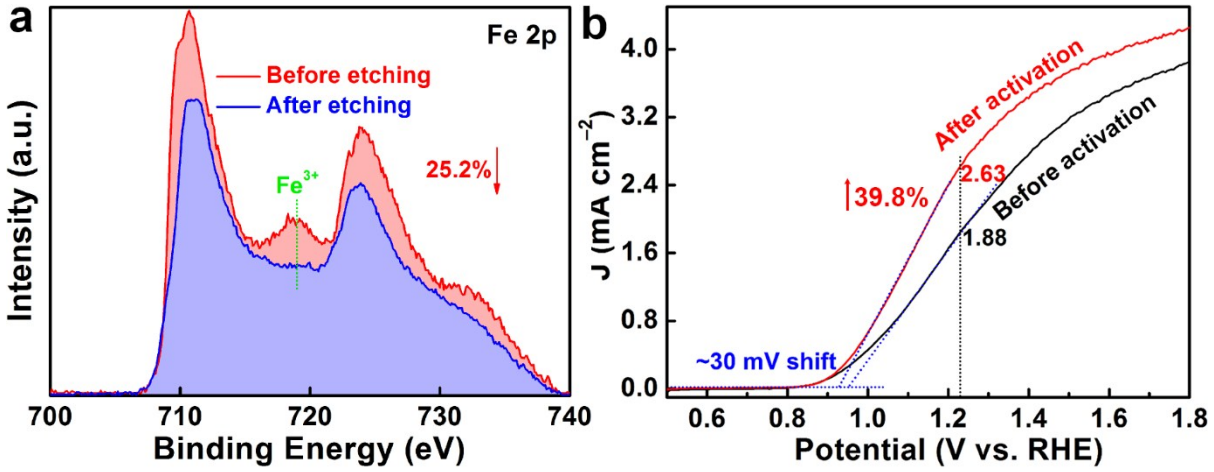

Fig. S11 Fe 2p XPS spectra (a) of activated sample before and after 300 s surface etching (~5 nm) using a reversed activation process (initial thrice anodic scanning followed by thrice cathodic scanning), and corresponding *J*–*V* curves (b).

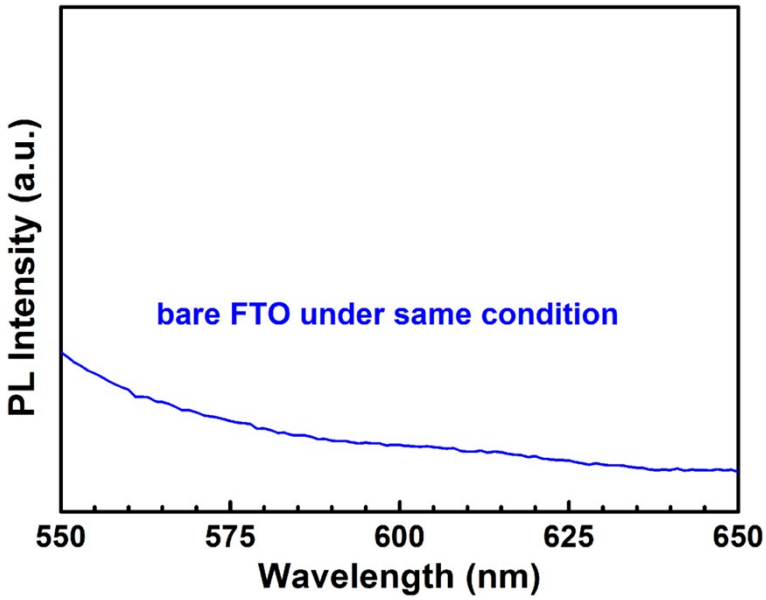

Fig. S12 PL of bare FTO under same synthesized condition as hematite.

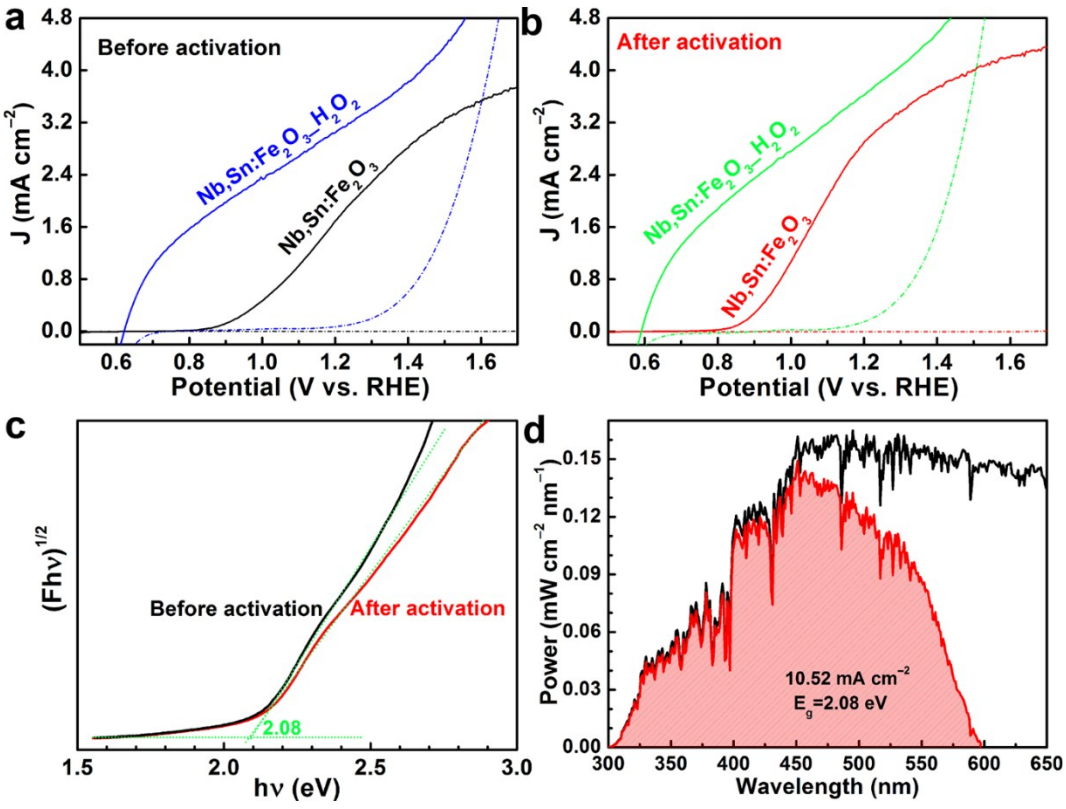

Fig. S13 *J–V* curves measured in 1 M KOH electrolyte with and without addition of 0.5 M H_2O_2 (a, pristine hematite. b, hematite after activation). (c) The derived bandgap from corresponding UV-vis absorption (Fig. 1d). (d) Light harvesting efficiency (LHE) of hematite corresponding to AM 1.5 G spectrum (Both are equal value because of almost same LHE and bandgap). Absorption photocurrents (J_{abs}): 10.52 mA cm^{-2}, <597 nm.

The obtained photocurrent density, J_{H_2O}, could be represented as following:

$$J_{H_2O} = J_{abs} \times \eta_{bulk} \times \eta_{surface} \quad (1)$$

Since there is no injection barrier of holes for H_2O_2 oxidation ($\eta_{surface} = 1$)

$$J_{H_2O_2} = J_{abs} \times \eta_{bulk} \quad (2)$$

Hence $$\eta_{surface} = J_{H_2O}/J_{H_2O_2} \quad (3)$$

And $$\eta_{bulk} = J_{H_2O_2}/J_{abs} \quad (4)$$

Here, $J_{H_2O_2}$ is the photocurrent density measured in 1 M NaOH with 0.5 M H_2O_2 and J_{abs} is the expected photocurrent density when absorbed photons are completely converted into current. For calculation of J_{abs}, the correlation between absorbance and irradiation is the following:[2]

$$P_d = P_0 10^{-A} \quad (5)$$

$$P_{abs} = P_0(1 - 10^{-A}) \quad (6)$$

P_0 (unit: mW cm^{-2} nm^{-1}) is power provided by solar simulator (in this case, AM 1.5G), P_{abs} is power of light actually absorbed by photoanode and P_d is power of light not absorbed at the photoanode but dissipated by reflection and penetration. A is absorbance of photoanode and LHE is defined as $1 - 10^{-A}$. So light not absorbed at the photoanode will be 10^{-A}. Integration of $P_{abs}(\lambda)$ (mW cm^{-2} nm^{-1}) along with wavelength λ gives total power density (unit of mW cm^{-2}), which is the power of light absorbed by photoanode (maximum power of photoanode). The following formula shows such relationship photon absorption (J_{abs}).

$$J_{abs}\left(\frac{mA}{cm^2}\right) = \int_{\lambda_1}^{\lambda_2} \frac{\lambda}{1240} P_{abs(\lambda)} d\lambda \left(\frac{mW}{cm^2}\right) \quad (7)$$

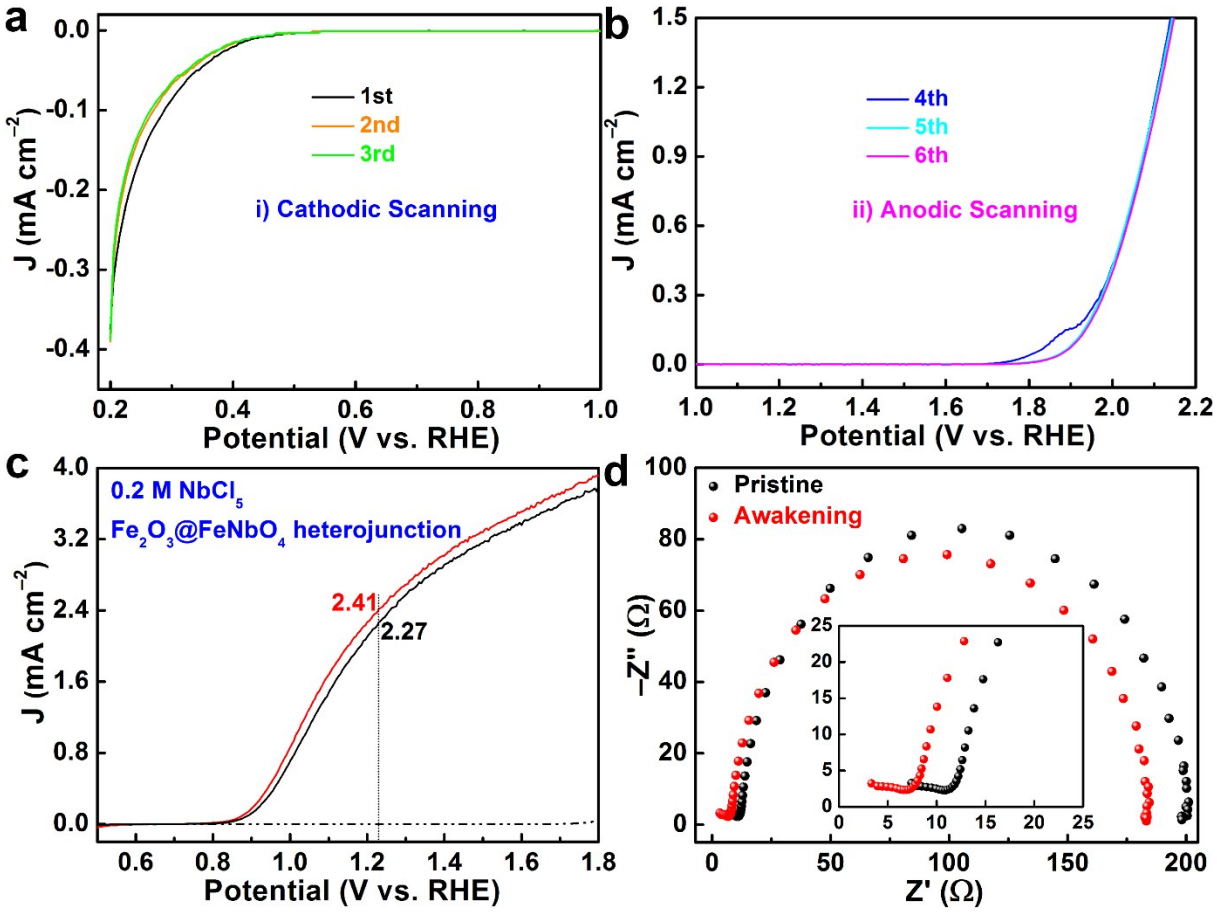

Fig. S14 Electrochemical activation of core-shell Fe_2O_3@$FeNbO_4$ heterojunction nanorods: a thrice cathodic scanning (a) and a following thrice anodic scanning (b). The corresponding *J*–*V* curves (c) and EIS (d) before and after activation.

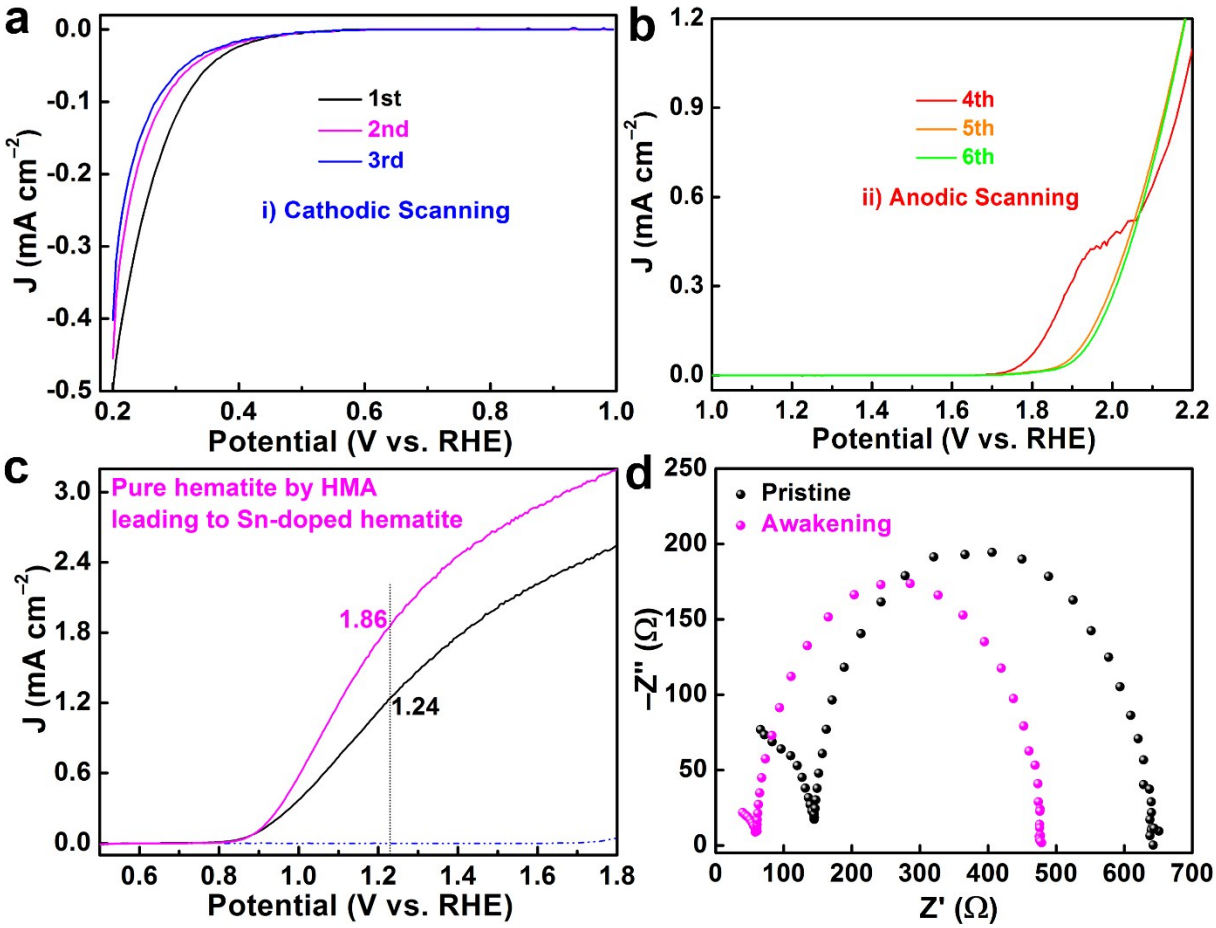

Fig. S15 Electrochemical activation of Sn-doped hematite nanorods: a thrice cathodic scanning (a) and a following thrice anodic scanning (b). The corresponding *J*–*V* curves (c) and EIS (d) before and after activation.

Table S1. Several samples of Nb,Sn:Fe_2O_3 photoanodes by electrochemical activation.

Nb,Sn:Fe_2O_3	Photocurrent (mA cm^{-2}) pristine→activated (percent)	Onset potential (V_{RHE}) pristine→activated (shift)
Sample 1	1.81→2.95 (62.9%↑)	0.98→0.90 (~80 mV)
Sample 2	1.79→2.93 (63.7%↑)	0.96→0.89 (~70 mV)
Sample 3	1.91→3.01 (57.6%↑)	1.00→0.94 (~60 mV)
Sample 4	1.88→3.05 (62.3%↑)	0.95→0.88 (~70 mV)

Table S2. The fitting results of EIS by Z-view software.

R (Ω) C (F)	R_s	R_{ct}	R_{trap}	C_{bulk}	C_{trap}
Before activation	33.2	88.4	201.1	1.85×10^{-8}	1.16×10^{-5}
After activation	28.8	58.9	99.2	7.78×10^{-8}	8.33×10^{-5}

Table S3. The fitting results of time-resolved PL by fitting software (FluoFit).

Samples	τ_{avg} [ns]	τ_1 [ns]	τ_2 [ns]	τ_3 [ns]	χ^2
Before activation	3.265	0.995 (39.50%)	3.482 (47.22%)	9.249 (13.28%)	1.04
After activation	3.494	0.883 (35.41%)	3.538 (49.57%)	9.498 (15.02%)	1.128

Table S4. Several samples of Nb,Sn:Fe_2O_3 photoanodes by electrochemical activation[1].

Nb,Sn:Fe_2O_3@$FeNbO_4$	Photocurrent (mA cm^{-2}) pristine→activated (percent)
Sample 1	2.20→2.33 (5.9%↑)
Sample 2	2.24→2.37 (5.8%↑)
Sample 3	2.27→2.41 (6.2%↑)

[1]Onset potential shifts were negligible.

Table S5. Several samples of Sn:Fe_2O_3 photoanodes by electrochemical activation.

Sn:Fe_2O_3	Photocurrent (mA cm^{-2}) pristine→activated (percent)	Onset potential (V_{RHE}) pristine→activated (shift)
Sample 1	1.19→1.74 (46.2%↑)	0.93→0.92 (~10 mV)
Sample 2	1.27→1.81 (42.5%↑)	0.94→0.94 (~0 mV)
Sample 3	1.24→1.86 (44.4%↑)	0.92→0.90 (~20 mV)

References:

(1) Yang, Y.; Forster, M.; Ling, Y.; Wang, G.; Zhai, T.; Tong, Y.; Cowan, A. J.; Li, Y., Acid Treatment Enables Suppression of Electron-Hole Recombination in Hematite for Photoelectrochemical Water Splitting. *Angew. Chem. Int. Ed.* **2016,** *55*, 3403-3407.

(2) Jeong, H. W.; Jeon, T. H.; Jang, J. S.; Choi, W.; Park, H., Strategic Modification of $BiVO_4$ for Improving Photoelectrochemical Water Oxidation Performance. *J. Phys. Chem. C* **2013,** *117*, 9104-9112.